Published in final edited form as:

J Immunol. 2024 January 15; 212(2): 346–354. doi:10.4049/jimmunol.2300210.

Mouse trophoblast cells have attenuated responses to TNFα and IFNγ and can avoid synergic cytotoxicity of the two cytokines

Mona Fendereski[*], **Hao Ming**[†], **Zongliang Jiang**[†], **Yan-Lin Guo**[*]

[*]Cell and Molecular Biology Program, University of Southern Mississippi, Hattiesburg, MS 39406

[†]Department of Animal Sciences, Genetics Institute, University of Florida, Gainesville, FL 32608

Abstract

TNFα and IFNγ are two inflammatory cytokines that play critical roles in immune responses, but they can also negatively affect cell proliferation and viability. In particular, the combination of the two cytokines (TNFα/IFNγ) synergistically causes cytotoxicity in many cell types. We recently reported that mouse embryonic stem cells (ESCs) isolated from the blastocyst stage embryo do not respond to TNFα and have limited response to IFNγ, thereby avoiding TNFα/IFNγ cytotoxicity. The current study expanded our investigation to mouse trophoblast stem cells (TSCs) and their differentiated trophoblasts (TSC-TBs), the precursors and the differentiated cells of the placenta, respectively. We report here that TNFα/IFNγ does not show the cytotoxicity to TSCs and TSC-TBs that otherwise effectively kills fibroblasts, similar to ESCs. Although ESCs, TSCs, and TSC-TBs are dramatically different in their growth rate, morphology, and physiological functions, nevertheless, they share a similarity in being able to avoid TNFα/IFNγ cytotoxicity. We propose that this unique immune property may serve as a protective mechanism that limits cytokine cytotoxicity in the blastocyst. With molecular and cellular approaches and genome-wide transcriptomic analysis, we have demonstrated that the attenuated NFκB and STAT1 transcription activation is a limiting factor that restricts the effect of TNFα/IFNγ on TSCs and TSC-TBs.

Keywords

trophoblast stem cells; embryonic stem cells; blastocyst; inflammatory cytokines; cytotoxicity

Introduction

It is estimated that about 30% of naturally fertilized eggs do not successfully implant (1). Dysregulated immune response in the uterus is an important factor that causes implantation failure (2). The blastocyst is the preimplantation embryo that consists of two major components: the inner cell mass (ICM) and the trophectoderm (TE). The ICM gives rise to the fetus while the TE contributes to the development of the placenta. Implantation of the blastocyst into the uterus represents the most critical moment for the initiation of pregnancy, but it also elicits immunological responses at the maternal–fetal interface. Inflammatory cytokines are necessary for implantation but could negatively affect embryo development if

Correspondence To: Yan-Lin Guo, Ph.D., Department of Biological Sciences, The University of Southern Mississippi, 118 College Drive # 5018, Hattiesburg, MS 39406, Tel: (601) 266-6018; Fax: (601) 266-5797; yanlin.guo@usm.edu.

dysregulated, such as under inflammatory and infectious conditions (3). Currently, we have limited knowledge about the immune properties of cells in the blastocyst and how they deal with immunological challenges under physiological and pathological conditions.

A series of our studies have demonstrated that embryonic stem cells (ESCs) derived from the ICM have attenuated innate immune responses. Specifically, they have attenuated responses to LPS, TNFα, and IL-1β (4–6) and fail to express type I IFNs in response to viral infection (7–11). Apparently, ESCs are immunologically different from differentiated somatic cells and have attenuated innate immune responses. Antiviral and inflammatory responses play central roles in providing the first line of defense as critical parts of innate immunity. At the cellular level, these responses are mainly mediated by toll-like receptors, nucleotide-binding oligomerization domain-like receptors, and retinoic acid–inducible gene I–like receptors that recognize different pathogenic agents, known as pathogen associated molecular patterns (12). Upon binding with their ligands, the aforementioned receptors activate transcription factors, such as interferon response factors (IRFs) and NFκB, leading to the production of IFNs and inflammatory cytokines that participate in different aspects of the immune response (13,14). IFNs bind to their cell surface receptors and activate the JAK-STAT pathway, leading to the expression of IFN-stimulated genes that promote the cell to enter an “antiviral state” (15). Inflammatory cytokines, such as TNFα, activate their specific receptors and lead to inflammatory responses (16). As the name indicates, cellular innate immunity is presumably developed in most, if not all, types of somatic cells in vertebrates. However, what has recently been found in ESCs suggests that innate immunity is not, at least not entirely, “innate” to ESCs, and the ability to mount IFN and inflammatory responses is acquired in somatic cells during differentiation as we demonstrated in ESC-differentiated fibroblasts (ESC-FBs) (9,17).

These findings in ESCs raise an intriguing question as to why these cells do not produce IFNs and have limited responses to certain inflammatory cytokines. We have discussed the biological implications of this phenomenon from different perspectives (18–21). From the perspective of immunology, immune response is viewed as a double-edged sword: it serves as a critical part of the defense mechanism but also causes collateral damage by inhibiting cell proliferation and causing cell death as a part of the immune response to eliminate infected or damaged cells (22–24). It is conceivable that immunological cytotoxicity could be tolerated in the tissue of a developed organism, but it could be detrimental to an early embryo. The cells in the blastocyst have a dedicated task of rapid proliferation for embryogenesis and could be particularly vulnerable. Indeed, excessive cytokine production of TNFα and IFNγ caused by systemic or reproductive tract inflammation and infection is recognized as a leading cause of implantation failure (25). In mice, LPS-induced production of TNFα and IFNγ dramatically increased the number of defected embryos (26,27). Therefore, TNFα and IFNγ are considered to be the major “embryotoxic cytokines” (25). It would be beneficial for cells in the blastocyst not to produce or respond to these cytokines resulting from implantation or intrauterine infection. At the cellular level, we have demonstrated that the combination of TNFα and IFNγ caused cell death of ESC-FBs, but it had no apparent effects on mouse and human ESCs and human induced pluripotent stem cells (4–6). These findings have led to our hypothesis that an attenuated

response to inflammatory cytokines in ESCs may serve as a protective mechanism to avoid immunological cytotoxicity (20,21).

The above hypothesis makes sense only if the attenuated innate immune response does not compromise ESCs' overall innate immunity. Indeed, recent studies suggest that ESCs have adapted alternative mechanisms to gain antiviral innate immunity, such as by using a subset of preexisting or intrinsic IFN-stimulated genes (28). We have recently reported that trophoblast stem cells (TSCs) isolated from the TE of the blastocyst and TSC-differentiated trophoblasts (TSC-TBs) can produce IFNs and provide antiviral activity to ESCs via paracrine signaling (29). TSCs and TSC-TBs also have altered glycosylation mechanisms that limit viral replication and infectivity (30). In this study, we extended our investigation to the responses of TSCs and TSC-TBs to TNFα and IFNγ. Our results demonstrate that TSCs and TSC-TBs are refractory to TNFα/IFNγ cytotoxicity like ESCs, and we discuss the biological implications of the unique immunological properties of the cells in the blastocyst.

Materials and Methods

Cells and cell culture

Mouse TSCs (provided by Dr. Wei Hsu, University of Rochester Medical Center) (31,32) were routinely maintained in medium that contains 70% mouse embryonic fibroblast (MEF)-conditioned medium (CM) and 30% basal TSC culture medium (RPMI 1640 containing 20% FBS, 1 mM sodium pyruvate, 2 mM L-glutamine, 50 units/mL penicillin, 50 μg/mL streptomycin, 0.1 μM 2-mercaptoethanol, 25 ng/mL Fibroblast Growth Factor (FGF4), and 1 μg/mL heparin). TSC differentiation was carried out according to published protocols (33). Briefly, TSCs were promoted to differentiate by withdrawing FGF4, heparin, and MEF-CM and were cultured in basal TSC culture medium for 5–6 days. The differentiated cells were designated as TSC-TBs. The culture conditions for ESC-FBs and MEFs were previously described (7). All cells were maintained at 37 °C in a humidified incubator with 5% CO_2.

Cell treatment

Cells at 60–70% confluence were treated with mouse TNFα and IFNγ (20 ng/ml, PeproTech, Rocky Hill, NJ) individually or in combination (TNFα/IFNγ). Cells were also treated with conditioned medium (CM) prepared from RAW cells (RAW 264.7 cells) that contains inflammatory cytokines as previously described (5). Briefly, RAW cells were treated with LPS (1 μg/ml, Sigma-Aldrich, St. Louis, MO) for 4 h. Then, the medium was removed, cells were washed three times with PBS, and fresh medium was added to the cells. After 24 h, the CM was collected and designated as LPS/CM. CM prepared from RAW cells without LPS treatment was used as control (Con/CM). The CM was diluted with 10% FBS DMEM (1:1) before it was used for cell treatment.

Real-time quantitative polymerase chain reaction (RT-qPCR)

Total RNA was extracted using TRI-reagent. cDNA was prepared using Moloney murine leukemia virus reverse transcriptase. RT-qPCR was performed using SYBR Green Ready Mix with an MX3000P RT-PCR system (Agilent, Santa Clara, CA). The mRNA levels from

RT-qPCR were calculated using the comparative Ct method. B-actin was used as a calibrator for the calculation of relative mRNA levels of the tested genes as previously described (7). As specified in individual experiments, the mRNA levels were either expressed as fold of activation, where the values in the controls were designated as 1 or expressed as relative levels normalized to β-actin. The sequences of the primer sets utilized for RT-qPCR are listed in Table I.

Cell viability analysis

Cell morphology and viability were routinely monitored with an Olympus CKX31 phase contrast microscope during the time course of treatment. Cell viability was determined by the number of viable cells after toluidine blue staining. The absorbance at 630 nm of toluidine blue extracted from the stained cells was measured with a BioTek ELx800 microtiter plate reader. The values, which correlate with the number of cells in the cell culture dish, were used as an indirect measurement of cell proliferation/viability (6).

Western-blot, immunocytochemistry, and microscopic analysis

Western-blot analysis was performed according to previously published methods (7). Anti-β-ACTIN antibodies (A5441) were purchased from Sigma-Aldrich (St Louis, MO). Antibodies against STAT1 (sc-417), inducible nitric oxide synthase (iNOS) (sc-7271), IκBα (sc-371), p-IκBα (sc-52943), TNFR1 (sc-8436) and m-IgGκ BP-HRP (sc-516102) were purchased from Santa Cruz Biotechnology (Dallas, TX). Antibodies against p-P65 (#3031), NFκB p65 (#8242), IRF1 (#8478), and anti-rabbit IgG HRP (#7074) were purchased from Cell Signaling Technology (Danvers, MA). Antibody against IFNγ receptor β chain (IFNGR2, Cat #559917) was purchased from BD Biosciences (San Jose, CA). Immunochemistry was performed according to our published methods with some modifications (28). Briefly, cells were fixed with 4% paraformaldehyde for 15 min and permeabilized in 4% FBS, 0.1% Triton-X 100 in PBS for 1 h at room temperature. Cells were incubated with antibodies against NFκB p65 or IRF1 and detected with secondary antibodies conjugated with fluorescein (FITC). The cells were then examined under a Leica Stellaris STED Super-Resolution Confocal Microscope.

RNA-seq analysis

TSCs, TSC-TBs, and MEFs treated with TNFα, IFNγ, or TNFα/IFNγ for 12 h were collected for RNA isolation using TRIzol (Thermo Fisher Scientific, Waltham, MA). RNA-seq libraries were prepared using the NEBNext RNA Library Prep Kit (New England Biolabs, Ipswich, MA) following the manufacturer's instructions. Briefly, poly(A) mRNA was isolated using the NEBNext poly(A) mRNA Magnetic Isolation Module. RNA-seq libraries were then constructed with NEBNext Ultra II RNA Library Prep Kit and multiplexed with NEBNext Multiplex Oligos for Illumina. The concentration of RNA-seq libraries was determined with a Qubit dsDNA HS Assay Kit (Thermo Fisher Scientific, Waltham, MA). The size of RNA-seq libraries was determined using the TapeStation 4200 system (Agilent Technologies, Santa Clara, CA). Pooled indexed libraries were then sequenced on the Illumina NovaSeq 6000 platform with 150-bp paired-end reads.

Multiplexed sequencing reads that passed filters were trimmed to remove low-quality reads and adaptors by Trim Galore (version 0.6.7) (-q 25 --length 20 --max_n 3 --stringency 3). The quality of reads after filtering was assessed by fastQC, followed by alignment to the mouse genome (GRCm39) by HISAT2 (version 2.2.1) with default parameters. The output SAM files were converted to BAM files and sorted using SAMtools6 (version 1.14). Read counts of all samples were quantified using featureCounts (version 2.0.1) with the mouse genome as a reference and were adjusted to provide CPM (counts per million mapped reads). The raw FASTQ files and normalized gene expression profiles (CPM) are available at Gene Expression Omnibus (GEO) (https://www.ncbi.nlm.nih.gov/geo/) under the accession number GSE224755.

Principal component analysis and cluster analysis were performed with R (a free software environment for statistical computing and graphics). Differentially expressed genes (DEGs) were identified using edgeR in R. Genes were considered differentially expressed if they provided a false discovery rate of <0.05 and fold change >2. ClusterProfiler was used to reveal the Gene Ontology (GO) and KEGG pathways in R.

Statistical analysis

Statistical analyses were performed using GraphPad Prism software (V.9) or Microsoft Excel Spreadsheet software. All experiments were repeated at least three times. Data are presented as the mean ± SD with three independent biological triplicates (n=3) in each experimental group, and differences were assessed for significance using two-tailed and unpaired Student's t test or one-way ANOVA. Statistical differences are indicated by p-values. P<0.05* was considered statistically significant.

Results

TSCs and TSC-TBs are less sensitive to cytokine cytotoxicity than MEFs and ESC-FBs

ESC-FBs and MEFs are mouse fibroblasts differentiated from ESCs in vitro and primary cells isolated from early embryos (day 11–13), respectively. Both are responsive to TNFα and IFNγ and were used for comparison with TSCs and TSC-TBs in this study. To determine cytokine toxicity, cells were treated with TNFα and IFNγ individually or in combination (TNFα/IFNγ) for 48 h. The number of cells in the cell culture dishes after treatment was used as an indirect measurement of cell viability. As shown in Fig.1A, TNFα or IFNγ alone had a limited but detectable effect on the viability of TSCs, TSC-TBs, MEFs, and ESC-FBs. However, the most notable observation is that TNFα/IFNγ significantly reduced the number of MEFs and ESC-FBs by ~60% and 80%, respectively, but it did not show additional cytotoxicity in TSCs and TSC-TBs when compared to treatment with TNFα or IFNγ alone (Fig.1A). Macrophages are a major type of innate immune cell capable of secreting a large amount of pro-inflammatory cytokines when stimulated with LPS, which mimics certain features of bacterial infection (34). We tested the responses of TSCs, TSC-TBs, and ESC-FBs to CM collected from LPS-activated RAW cells (LPS/CM), which contains various secreted inflammatory cytokines, including TNFα as we previously reported (5). LPS/CM caused significantly higher cytotoxicity in ESC-FBs than in TSCs and TSC-TBs (Fig. 1B). TSCs are characterized by their small size and clonal growth

while differentiated TSC-TBs have large-flattened cell bodies (Fig. 1C). We examined the effect of TNFα/IFNγ on morphology of TSCs, TSC-TBs, and MEFs. As shown in Fig. 1C, TNFα/IFNγ treatment did not show significant effects on TSC or TSC-TB morphology or cell viability, but it caused cell death of many MEFs that eventually detached from the culture dish, similar to the effect of TNFα/IFNγ on ESC-FBs as we previously described (6). These results suggested that TSCs and TSC-TBs have higher tolerance to cytokine cytotoxicity than fibroblasts. The rest of our study focused on investigating the responses of TSCs and TSC-TBs to TNFα and IFNγ in comparison with MEFs or TSC-TBs.

TNFα induced limited NFκB activation and inflammatory gene expression in TSCs and TSC-TBs

To determine cellular response to TNFα, we first analyzed TNFα-induced expression of ICAM1 and IL6, which are commonly used as indications of TNFα-induced inflammatory response (35,36). As shown in Fig. 2A, TNFα induced significantly increased ICAM1 and IL6 mRNA expression in MEFs (~5- and 8-fold, respectively), but its effects on TSCs and TSC-TBs were negligible. The lack of expression of the two genes was confirmed in TSCs and TSC-TBs that were treated for different time periods up to 48 h with a dose of TNFα up to 100 ng/ml (data not shown). TNFα-induced genes are mainly regulated by the transcription factor NFκB. In resting cells, NFκB is retained in the cytoplasm by binding to inhibitor of NFκB protein (IκB). Upon cell activation, IκB is degraded and the freed NFκB is translocated to the nucleus where it activates transcription of target genes. These processes require phosphorylation of IκBα and the p65 subunit of NFκB. As shown in Fig. 2B, phosphorylation of IκBα and p65 (detected by p-IκBα and p-p65, respectively) was detected during a time course with TNFα treatment from 15 min to 60 min in ESC-FBs. Specifically, IκBα was degraded at 15 min and 30 min (indicated by reduced band intensity) followed by a recovery at 60 min, and phosphorylation of IκBα and p65 increased at 15 min and 30 min. However, these changes were not observed in TNFα−treated TSCs and TSC-TBs. To ascertain the effect of TNFα on NFκB activation, we further analyzed nuclear translocation of p65, which is another commonly used indicator of NFκB activation (37). In control cells, NFκB was mainly detected in the cytoplasm. TNFα treatment did not cause apparent change in TSCs, but it induced NFκB nuclear translocation in a few TSC-TBs (Fig. 2C). In MEFs, on the other hand, nearly all cells became NFκB nuclear positive in TNFα-treated cells (Fig. 2C). These results further confirm that NFκB is not or is minimally activated in TSCs and TSC-TBs, which could explain the lack of TNFα-induced transcription of *Il6* and *Icam1* (Fig.2A).

Comparative analysis of TNFα−induced gene expression in TSCs, TSC-TBs, and MEFs by RNA sequencing (RNA-seq)

To have a comprehensive analysis of TNFα-induced gene expression changes, we performed RNA-seq analysis of TSCs, TSC-TBs, and MEFs that were treated with TNFα for 12 h. As shown in Fig.3A, TNFα induced a large number of differentially expressed DEGs in MEFs. However, the numbers of up- and down-regulated DEGs by TNFα and their magnitudes of responses in TSCs and TSC-TBs were substantially lower than in MEFs. We compared the relative expression levels of the key signaling molecules in the TNFα pathway, including TNF receptors (*Tnfrsf1a* and *Tnfrsf1b*), the signal transducers/regulators (*Bag4, Tradd,*

Traf2, Mapk3k14, Ripk1, Ripk2, and *Mlk1*), and the signaling components of the NFκB branch (*Ikbkb, Ikbke, Nfkb1, Nfkb2, RelA/p65, RelB, Nfkbia,* and *Usp4*) (Fig. 3B). The expression level of TNF receptor 1 (TNFR1 encoded by *Tnfrsf1a*), the major receptor that mediates the effect of TNFα, is expressed at the lowest level in TSCs. Its expression level is notably increased in TSC-TBs but is still lower than in MEFs. On the other hand, *Bag4*, which encodes SODD, a major negative regulator of the TNFα pathway (38), is expressed at a higher level in TSCs and TSC-TBs. Except for *Nfkb2* and *Ikbkb*, all other signaling components in the NFκB pathways were expressed at substantially lower levels in TSCs and/or TSC-TBs than in MEFs (Fig. 3B). These results could, at least partly, explain attenuated activation of the NFκB pathway in TSCs and TSC-TBs by TNFα. This is further confirmed by the quantitative analysis of several genes commonly involved in inflammatory responses (*Il1a, Icam1, Cxcl10, Nod2, and Tlr2*), all of which were significantly upregulated by TNFα in MEFs. Except for *Icam1* mRNA, which was slightly upregulated in TSCs, TNFα did not show apparent effects on all other genes tested in TSCs and TSC-TBs (Fig. 3C). The results from RNA-seq are in line with the lack of *Icam1* and *Il6* mRNA induction determined by RT-qPCR (Fig. 2A). The expression levels of inflammatory genes in TSCs, TSC-TBs, and MEFs are well correlated with the levels of NFκB activation shown in Fig. 2, i.e., NFκB is strongly activated in MEFs but minimally or not activated in TSCs and TSC-TBs. While TNFR1 along with several other signaling molecules are upregulated in TSC-TBs after differentiation from TSCs, NFκB activation was not significantly increased. It is likely that NFκB activation in TSC-TBs is restricted by other yet to be identified mechanisms.

IFNγ-induced responses in TSCs, TSC-TBs, MEFs, and ESC-FBs

IFNγ induces cellular responses mainly through its cell surface receptor complex that consists of IFNGR1 and IFNGR2. The receptor complex then activates tyrosine kinases JAK1 and JAK2, which in turn activate STAT1, leading to IFNγ-induced gene transcription. *Irf1* is an early IFNγ response gene that activates the transcription of a large number of secondary response genes. STAT1 itself is also upregulated by IFNγ as a positive feedback regulatory mechanism (39,40). Using the induction of these two genes as an indicator of IFNγ-induced responses, we demonstrated that IFNγ could induce *Stat1* and Irf1 mRNA in TSCs, TSC-TBs, MEFs, and ESC-FBs at different levels (Fig. 4A). IFNγ-induced STAT1 was further demonstrated by Western-blot (Fig. 4B, IFNα- and IFNλ-induced STAT1 was also tested for comparison). Similarly, IFNγ-induced IRF1 protein was also readily detected in TSCs, TSC-TBs, and ESC-FBs by Western-blot (data not shown). Immunostaining analysis revealed that IFNγ-induced IRF1 was accumulated in the nuclei of TSCs and TSC-TBs, as expected for a transcription factor (Fig. 4C). It is noted that the data in Fig.4A are presented as the fold activation of STAT1 and IRF1. While these results clearly demonstrated the responsiveness of the cells to IFNγ, they did not reflect the relative expression levels of the two genes in the three cell types. Therefore, we analyzed the relative expression levels of STAT1 and IRF1 in the control cells and in IFNγ-treated MEFs, TSCs, and TSC-TBs using RNA-seq. As shown in Fig.4D, IFNγ could induce transcription of both STAT1 and IRF1 in TSCs and TSC-TBs, but the levels of their induction are much lower than in MEFs.

We further analyzed IFNγ-induced gene expression profiles based on RNA-seq data. The numbers of up- and down-regulated DEGs and their magnitude of changes in MEFs are significantly higher than in TSCs and TSC-TBs (Fig. 5A). The relative expression levels of the key molecules in the IFNγ-pathway were illustrated in a heat map (Fig 5B), including cell-surface receptors (*Ifngr1 and Ifngr2*), signal transducers (*Jak1, Jak2, and Stat1*), and negative regulators (*Socs1, Socs3, and Ptpn6*). Among these genes, *Ifngr1, Ifngr2, and Jak1* were expressed at the lowest levels in TSCs. Their expression levels were slightly higher in TSC-TBs than in TSCs but were still much lower than in MEFs. Conversely, the negative regulator, *Ptpn6*, was expressed at higher levels in TSCs and TSC-TBs than in MEFs. It is also noted that both positive regulators (*Jak2 and Stat1)* and negative regulators (*Socs1, Socs3, and Ptpn6)* were upregulated in TSC-TBs after differentiation (Fig 5B). To further determine the cellular response levels to IFN γ, we quantitatively analyzed several common IFN γ-induced genes, including transcription factors (*Stat1 and Irf8*), antiviral/antimicrobial defense genes (*Gbp7 and Nos2*), and genes associated with major histocompatibility complex proteins (*B2m and Tapbp*). The results show a clear pattern that IFN γ induced the strongest responses in MEFs among the three cell types while the responses in TSC-TBs are slightly higher than in TSCs (Fig. 5C). These results correlate with the expression levels of signaling molecules (Fig. 5B) and the numbers and transcription levels of IFN γ-induced DEGs in the three cell types (Fig. 5A).

TNFα and IFNγ synergistically induce iNOS in MEFs and ESC-FBs but not in TSCs and TSC-TBs

It is known that TNFα and IFNγ synergistically induce certain genes with promoters that have binding sites for both NFκB and STAT1 (39,40). iNOS (encoded by *Nos2*) is one such gene that causes synergistic TNFα/IFNγ cytotoxicity in many cell types, including ESC-FBs as we recently reported (6). As shown in Fig.6A, *Nos2* mRNA was induced ~10- and 50-fold by IFNγ alone in MEFs and ESC-FBs, respectively. The combination of the two cytokines (TNFα/IFNγ) caused ~70- and 400-fold increase of *Nos2* mRNA in MEFs and ESC-FBs, respectively. The strong induction of iNOS protein by TNFα/IFNγ was readily detected by Western-blot analysis in ESC-FBs and MEFs, but not in TSCs and TSC-TBs (Fig.6B). The expression levels of iNOS correlate well with the cytotoxicity of TNFα/IFNγ as described in TSCs, TSC-TBs, MEFs, and ESC-FBs in Fig.1A. Furthermore, the mRNA levels of iNOS induced by TNFα, IFNγ, and TNFα/IFNγ determined from RNA-seq mirror the RT-qPCR results (Fig.6C). It is interesting that IFNγ could induce a slight increase of *Nos2* mRNA in TSC-TBs, but TNFα, either alone or in combination with IFNγ, did not induce iNOS expression or cause additional effects on iNOS expression in both TSCs and TSC-TBs (Fig.6C). Apparently, the synergy between TNFα and IFNγ displayed in MEFs and ESC-FBs did not take place in TSCs and TSC-TBs in any of the above-mentioned experiments (Fig.1A and Fig.6A, B, and C). We further analyzed the baseline expression of IFNGR2 and TNFR1 by Western blot. The result showed their protein levels are lower in TSCs and TSC-TBs than in MEFs, which further explains the attenuated responses of TSCs and TSC-TBs to TNFα and IFNγ and the lack of synergy between the two cytokines in inducing iNOS in these cells.

The lack of synergy between TNFα and IFNγ is common to all upregulated DEGs in TSCs and TSC-TBs

We further analyzed the commonly upregulated DEGs in TSCs, TSC-TBs, and MEFs treated with TNFα, IFNγ, and TNFα/IFNγ. RNA-seq data revealed that there are 1, 18, and 24 DEGs commonly upregulated by treatment with TNFα, IFNγ, and TNFα/IFNγ, respectively, in the three cell types. There were 890 upregulated DEGs in MEFs treated with TNFα/IFNγ, which was more than the sum of upregulated genes by TNFα and IFNγ alone (387 and 285, respectively), suggesting synergistic effects of the two cytokines. In contrast, the numbers of upregulated DEGs in TSCs and TSC-TBs receiving TNFα/IFNγ were rather similar to the number of DEGs upregulated by IFNγ alone (Fig.S1). In MEFs, most of the DEGs are expressed at higher levels in TNFα/IFNγ-treated cells than in the cells treated with TNFα or IFNγ alone (e.g., *Il1rl1, Mmp3, Ccl2*), representing the genes that were synergistically upregulated by TNFα and IFNγ. A few genes were expressed at similar levels in TNFα/IFNγ- and IFNγ-treated MEFs (e.g., *Igtp and Gab7),* which represent the genes that are induced by IFNγ alone. Analysis of commonly upregulated DEGs in TSCs and TSC-TBs revealed that all genes upregulated by TNFα/IFNγ and IFNγ alone were expressed at similar levels in TSCs and TSC-TBs, a similar pattern to iNOS described in Fig.6C. A simple interpretation would be that the synergistic action between TNFα and IFNγ in MEFs resulted in additional DEGs and that this phenomenon did not happen in TSCs and TSC-TBs.

Discussion

In a previous study, we demonstrated that TSCs and TSC-TBs have a functional IFN system that can produce IFNs and protect ESCs from viral infection (29). This finding suggests that the TE, as the precursor of the placenta, can provide antiviral protection to the early embryo even at the blastocyst stage. In this study, we extended our investigation to the responses of TSCs and TSC-TBs to inflammatory cytokines. Our findings demonstrate that TSCs and TSC-TBs have limited responses to TNFα and IFNγ, which may serve as a unique mechanism to limit cytotoxicity associated with inflammatory responses.

We previously reported that both human and mouse ESCs have attenuated responses to TNFα and IFNγ and can avoid the TNFα/IFNγ cytotoxicity that can kill naturally differentiated fibroblasts and ESC-FBs (4–6). The current study demonstrates that TSCs and TSC-TBs share this similarity with ESCs with similar underlying molecular mechanisms, including the low-level expression of cytokine receptors and some key signaling molecules and higher expression levels of negative regulators that mediate the effects of TNFα and IFNγ. Most of the signaling molecules in the TNFα and IFNγ pathways are notably upregulated in TSC-TBs at the mRNA levels after differentiation as indicated by RNA-seq data. However, these changes did not result in an apparent increase in cellular response of TSC-TBs to TNFα. Although TSC-TBs have notably increased responses to IFNγ in comparison with TSCs, their response levels are still significantly lower than in MEFs. It is interesting to note that the findings in TSC-TBs vs. TSCs are very different from those in ESC-FBs vs. ESCs, in which ESC-FBs gain increased responsiveness to TNFα and IFNγ and become highly susceptible to the cytotoxicity of TNFα/IFNγ after differentiation (5,6).

The molecular mechanisms underlying the attenuated responses of TSCs and TSC-TBs to TNFα and IFNγ are not completely understood, but it is apparent that the restrictions are at multiple levels, including the expression levels of receptors, signaling molecules, and negative regulators. It is noted that the signaling pathway that mediates the effects of IFNγ is clearly functional in TSCs and TSC-TBs and showed much stronger response to IFNγ than ESCs (6). iNOS is a mediator of TNFα/IFNγ cytotoxicity. iNOS can produce a large amount of nitric oxide, which is an important immune defense molecule but also a free radical that can cause cellular damage (41,42). Synergistic induction of iNOS by TNFα/IFNγ depends on co-activation of NFκB and STAT1. Nevertheless, the synergistic action between NFκB and STAT1, which is essential for iNOS induction, does not occur in TSCs and TSC-TBs due to the lack of NFκB activation, thus preventing the cytotoxicity resulting from synergistic action of TNFα and IFNγ as observed in fibroblasts. The lack of iNOS induction from TNFα/IFNγ treatment in ESCs is attributed to inactivity of NFκB and STAT1, as we previously demonstrated (6). The data presented in this study also suggests that this is likely the case for TSCs and TSC-TBs.

The transcriptomic RNA-seq analysis provides a holistic view of TNFα-, IFNγ-, and TNFα/IFNγ-induced genes that further support our conclusions. As expected, a large number of the DEGs identified in MEFs are related to immune responses and signaling molecules that mediate antiviral and inflammatory responses. The genes in this category identified in TSCs and TSC-TBs are expressed at substantially lower levels than in MEFs under the same treatment conditions, confirming the overall lower level of immune responses in these cells. Furthermore, RNA-seq analysis revealed a large number of genes that are synergistically upregulated by TNFα/IFNγ in MEFs, including iNOS which we previously characterized in ESC-FBs (6) and now in this study. In TSCs and TSC-TBs, TNFα/IFNγ induced gene expression was basically attributed to the effect of IFNγ alone since TNFα did not cause additional effects as it did in MEFs. While the significance of low-level responses of TSCs and TSC-TBs to IFNγ remains to be investigated, it is tempting to speculate that IFNγ-induced defense genes could contribute to the innate immunity of these cells against microbial pathogens. It should be pointed out we did not analyze the DEGs other than those involved in the immune response induced by TNFα, IFNγ, or TNFα/IFNγ. Other DEGs in TSCs and TSC-TBs, although expressed at low levels, could be biologically significant in different ways such as those related to tissue invasion or vascular development (43,44) and will need further investigation with additional experimental approaches.

ESCs, TSCs, and TSC-TBs dramatically differ in their growth rate, morphology, and physiological functions. Nevertheless, they share a similarity in their ability to avoid the cytotoxicity of TNFα/IFNγ. While the physiological implications of this remain to be further elucidated, we propose that the attenuated response to TNFα/IFNγ in the TE may help to minimize inflammatory toxicity and makes the blastocyst “an immune-privileged structure.” In this way, the blastocyst can avoid immunological cytotoxicity associated with implantation and inflammatory conditions, which could be an adaptive feature for normal growth and development of an early embryo in an immunologically challenging environment.

Supplementary Material

Refer to Web version on PubMed Central for supplementary material.

Acknowledgments

We thank Dr. Wei Hsu (University of Rochester Medical Center) for providing TSCs. We also thank Mississippi-IDeA Network of Biomedical Research Excellence for the use of the imaging facility (funded by the National Institute of General Medical Sciences P20 GM103476-11).

This work was in part supported by the National Institute of General Medical Sciences (R15GM128196, YLG) and the NIH Eunice Kennedy Shriver National Institute of Child Health and Human Development (R01HD102533, ZJ) and USDA National Institute of Food and Agriculture (2019-67016-29863, ZJ).

Abbreviations used in this article:

ESCs	embryonic stem cells
ICM	inner cell mass
TE	trophectoderm
TSCs	trophoblast stem cells
TSC-TBs	TSC-differentiated trophoblasts
ESC-FBs	ESC-differentiated fibroblasts
MEFs	mouse embryonic fibroblasts
CM	conditioned medium
IRFs	interferon response factors
IFGR2	IFNγ receptor β chain
RNA-seq	RNA sequencing
CPM	counts per million mapped reads
DEGs	Differentially expressed genes
iNOS	inducible nitric oxide synthase

References

1. Norwitz ER, Schust DJ, and Fisher SJ 2001. Implantation and the survival of early pregnancy. N Engl J Med 345: 1400–1408. [PubMed: 11794174]
2. Koot YEM, Teklenburg G, Salker MS, Brosens JJ, and Macklon NS 2012. Molecular aspects of implantation failure. Biochem Biophys Acta (BBA) - Molecular Basis of Disease 1822: 1943–1950.
3. Mor G, Aldo P, and Alvero AB 2017. The unique immunological and microbial aspects of pregnancy. Nat Rev Immunol 17: 469–482. [PubMed: 28627518]
4. D'Angelo W, Gurung C, Acharya D, Chen B, Ortolano N, Gama V, Bai F, and Guo Y-L 2017. The Molecular basis for the lack of inflammatory responses in mouse embryonic stem cells and their differentiated cells. J Immunol 198: 2147–2155. [PubMed: 28130495]

5. D'Angelo W, Chen B, Gurung C, and Guo Y-L 2018 Characterization of embryonic stem cell-differentiated fibroblasts as mesenchymal stem cells with robust expansion capacity and attenuated innate immunity. Stem Cell Res Ther 9: 278. [PubMed: 30359317]
6. Chen B, Chandan G, Guo J, Kwon C, and Guo Y-L 2020. Pluripotent stem cells are insensitive to the cytotoxicity of TNFα and IFNγ. J Reprod 160: 547–560.
7. Wang R, Wang J, Paul AM, Acharya D, Bai F, Huang F, and Guo Y-L 2013. Mouse embryonic stem cells are deficient in type I interferon expression in response to viral infections and double-stranded RNA. J Biol Chem 288: 15926–15936. [PubMed: 23580653]
8. Wang R, Wang J, Acharya D, Paul AM, Bai F, Huang F, and Guo Y-L 2014. Antiviral responses in mouse embryonic stem cells: differential development of cellular mechanisms in type I interferon production and response. J Biol Chem 289: 25186–25198. [PubMed: 24966329]
9. Wang R, Teng C, Spangler J, Wang J, Huang F, and Guo Y-L 2014. Mouse embryonic stem cells have underdeveloped antiviral mechanisms that can be exploited for the development of mRNA-mediated gene expression strategy. Stem Cells Dev 23: 594–604. [PubMed: 24219369]
10. Yu J, Rossi R, Hale C, Goulding D, and Dougan G 2009. Interaction of enteric bacterial pathogens with murine embryonic stem cells. Infect Immunity 77: 585–597. [PubMed: 19029302]
11. Wash R, Calabressi S, Franz S, Griffiths SJ, Goulding D, Tan E-P, Wise H, Digard P, Haas J, Efstathiou S, and Kellam P 2012. Permissive and restricted virus infection of murine embryonic stem cells. J Gen Virol 93: 2118–2130. [PubMed: 22815272]
12. Newton K, and Dixit VM 2012. Signaling in innate immunity and inflammation. Cold Spring Harb Perspect Biol 4: a006049. [PubMed: 22296764]
13. Kawai T, and Akira S 2011. Toll-like Receptors and their crosstalk with other innate receptors in infection and immunity. Immunity 34: 637–650. [PubMed: 21616434]
14. Kato H, Takahasi K, and Fujita T 2011. RIG-I-like receptors: cytoplasmic sensors for non-self RNA. Immunol Rev 243: 91–98. [PubMed: 21884169]
15. Schoggins JW, Wilson SJ, Panis M, Murphy MY, Jones CT, Bieniasz P, and Rice CM 2011. A diverse range of gene products are effectors of the type I interferon antiviral response. Nature 472: 481–485. [PubMed: 21478870]
16. Wajant H, Pfizenmaier K, and Scheurich P 2003. Tumor necrosis factor signaling. Cell Death Differ 10: 45–65. [PubMed: 12655295]
17. D'Angelo W, Acharya D, Wang R, Wang J, Gurung C, Chen B, Bai F, and Guo Y-L (2016) Development of antiviral innate immunity during in vitro differentiation of mouse embryonic Stem Cells. Stem Cells Dev 25: 648–659. [PubMed: 26906411]
18. Guo Y-L, Carmichael GG, Wang R, Hong X, Acharya D, Huang F, and Bai F 2015. Concise Reviews: attenuated innate immunity in embryonic stem cells and its implications in developmental biology and regenerative medicine. Stem Cells 33: 3165–3173. [PubMed: 26086534]
19. Guo Y-L 2017. Utilization of different antiviral mechanisms by mammalian embryonic stem cells and differentiated cells. Immunol Cell Biol 95: 17–23. [PubMed: 27485807]
20. Guo Y-L 2019. The underdeveloped innate immunity in embryonic stem cells: The molecular basis and biological perspectives from early embryogenesis. Am J Reprod Immunol 81: e13089. [PubMed: 30614149]
21. Guo Y-L, Gurung C, Fendereski M, and Huang F 2022. Dicer and PKR as novel regulators of embryonic stem cell fate and antiviral innate immunity. J Immunol 208: 2259–2266. [PubMed: 35577384]
22. Hertzog PJ, Hwang SY, and Kola I 1994. Role of interferons in the regulation of cell proliferation, differentiation, and development. Mol Reprod Dev 39: 226–232. [PubMed: 7530016]
23. Garcia MA, Meurs EF, and Esteban M 2007. The dsRNA protein kinase PKR: virus and cell control. Biochimie 89: 799–811. [PubMed: 17451862]
24. Samuel CE 2001. Antiviral actions of interferons. Clin Microbiol Rev 14: 778–809. [PubMed: 11585785]
25. Robertson SA, Chin PY, Femia JG, and Brown HM 2018. Embryotoxic cytokines-potential roles in embryo loss and fetal programming. J Reprod Immunol 125: 80–88. [PubMed: 29306096]

26. Kohmura Y, Kirikae T, Kirikae F, Nakano M, and Sato I 2013. Lipopolysaccharide (LPS)-induced intra-uterine fetal death (IUFD) in mice is principally due to maternal cause but not fetal sensitivity to LPS. Microbiol Immunol 44: 897–904.
27. Chin PY 2014. Cytokines and programming the preimplantation embryo paediatrics and reproductive health University of Adelaide, Australia. Thesis.
28. Wu X, Dao Thi VL, Huang Y, Billerbeck E, Saha D, Hoffmann HH, Wang Y, Silva LAV, Sarbanes S, Sun T, Andrus L, Yu Y, Quirk C, Li M, MacDonald MR, Schneider WM, An X, Rosenberg BR, and Rice CM 2018. Intrinsic immunity shapes viral resistance of stem cells. Cell 172: 423–438. [PubMed: 29249360]
29. Fendereski M, Neupane B, Nazneen F, Bai F, and Guo YL 2022. Mouse trophoblast cells can provide IFN-based antiviral protection to embryonic stem cells via paracrine signaling. J Immunol 208: 2761–2770. [PubMed: 35649628]
30. Neupane B, Fendereski M, Nazneen F, Guo YL, and Bai F 2021. Murine trophoblast stem cells and their differentiated cells attenuate zika virus in vitro by reducing glycosylation of the viral envelope protein. Cells 10: 3085 [PubMed: 34831310]
31. Chiu SY, Asai N, Costantini F, and Hsu W 2008 SUMO-specific protease 2 is essential for modulating p53-Mdm2 in development of trophoblast stem cell niches and lineages. PLOS Biology 6: e310. [PubMed: 19090619]
32. Maruyama EO, Lin H, Chiu SY, Yu H-MI, Porter GA, and Hsu W 2016. Extraembryonic but not embryonic SUMO-specific protease 2 is required for heart development. Sci Rep 6: 20999. [PubMed: 26883797]
33. Tanaka S, Kunath T, Hadjantonakis AK, Nagy A, and Rossant J 1998. Promotion of trophoblast stem cell proliferation by FGF4. Science 282: 2072–2075. [PubMed: 9851926]
34. Ramana KV, Fadl AA, Tammali R, Reddy ABM, Chopra AK, and Srivastava SK 2006. Aldose reductase mediates the lipopolysaccharide-induced release of inflammatory mediators in RAW264.7 murine macrophages. J Biol Chem 281: 33019–33029. [PubMed: 16956889]
35. Ledebur HC, and Parks TP 1995. Transcriptional regulation of the intercellular adhesion molecule-1 gene by inflammatory cytokines in human endothelial cells: essential roles of a variant NFkB site and p65 homodimers. J Biol Chem 270: 933–943. [PubMed: 7822333]
36. Libermann TA, and Baltimore D 1990. Activation of interleukin-6 gene expression through the NF-kappa B transcription factor. Mol Cell Bio.l 10: 2327–2334.
37. Guo Y-L, Kang B, Yang LJ, and Williamson JR (1999) Tumor necrosis factor-alpha and ceramide induce cell death through different mechanisms in rat mesangial cells. Am J Physiol 276: F390–F397. [PubMed: 10070162]
38. Takada H, Chen N, Mirtsos C, Suzuki S, Suzuki N, Wakeham A, Mak TW, and Yeh W 2003. Role of SODD in regulation of tumor necrosis factor responses. Mol Cell Biol 23: 4026–4033. [PubMed: 12748303]
39. Ohmori Y, Schreiber RD, and Hamilton TA (1997) Synergy between interferon-γ; and tumor necrosis factor-α; in transcriptional activation is mediated by cooperation between signal transducer and activator of transcription 1 and nuclear factor-kB. J Biol Chem 272: 14899–14907. [PubMed: 9169460]
40. Feng H, Zhang YB, Gui JF, Lemon SM, and Yamane D 2021. Interferon regulatory factor 1 (IRF1) and anti-pathogen innate immune responses. PLOS Pathogens 17: e1009220. [PubMed: 33476326]
41. Fauskanger M, Haabeth OAW, Skjeldal FM, Bogen B, and Tveita AA 2018. Tumor killing by CD4+ T cells is mediated via induction of inducible nitric oxide synthase-dependent macrophage cytotoxicity. Front Immunol 9: 1684. [PubMed: 30083157]
42. Korhonen R, Lahti A, and and HK 2005. Nitric oxide production and signaling in inflammation. Curr Drug Targets 4: 471–479.
43. Ashkar AA, Di Santo JP, and Croy BA 2000. Interferon γ Contributes to initiation of uterine vascular modification, decidual integrity, and uterine natural killer cell maturation during normal murine pregnancy. J Exp Med 192: 259–270. [PubMed: 10899912]
44. Otun HA, Lash GE, Innes BA, Bulmer JN, Naruse K, Hannon T, Searle RF, and Robson SC 2011. Effect of tumour necrosis factor-α in combination with interferon-γ on first trimester extravillous trophoblast invasion. J Reprod Immunol 88: 1–11. [PubMed: 21112094]

Key Points:

1. TSCs and TSC-TBs have attenuated responses to TNFα and IFNγ.
2. TSCs and TSC-TBs can avoid synergic cytotoxicity of TNFα and IFNγ.
3. An attenuated inflammatory response protects embryonic cells from cytokine toxicity.

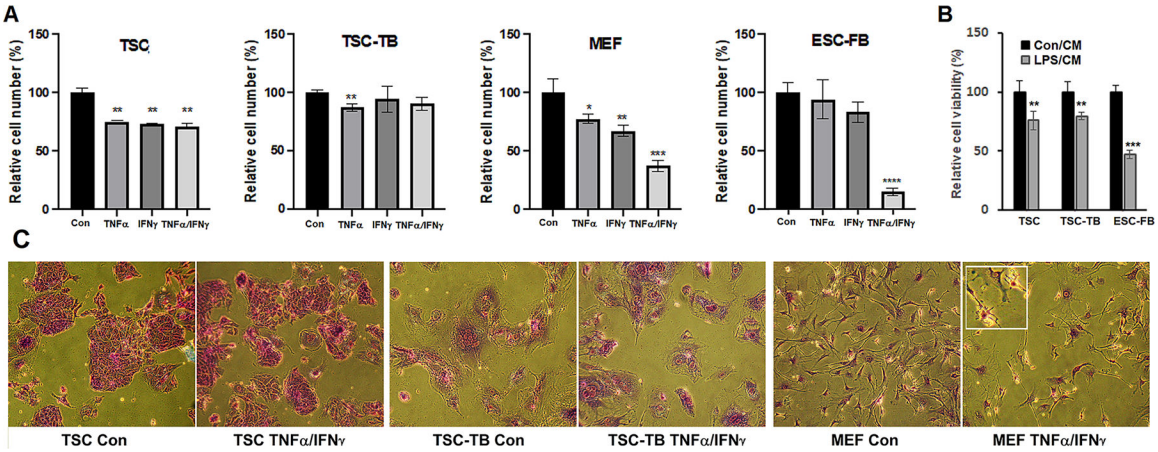

Fig. 1. TSCs and TSC-TBs are less sensitive to cytokine cytotoxicity than MEFs and ESC-FBs.

A, Cells were treated with TNFα, IFN γ, or TNFα/IFN γ. **B,** Cells were treated with conditioned medium from untreated RAW cells (Con/CM) or LPS-treated RAW cells (LPS/CM). Cell viability in **A** and **B** was determined by toluidine blue staining of cells treated for 48 h. Cell number in the control group (**A,** Con; **B,** Con/CM) was defined as 100%. Values are mean ± SD (n=3). P<0.0001, ****, P<0.001, ***; P<0.01, **; P<0.05, * compared with the control group. **C,** TSCs, TSC-TBs, and MEFs were treated with TNFα/IFN γ for 48 h. Cells were fixed and stained with toluidine blue and photographed under a phase contrast microscope (100x magnification). The square inset denotes an enlarged image of two dying MEFs that were about to detach from the culture dish.

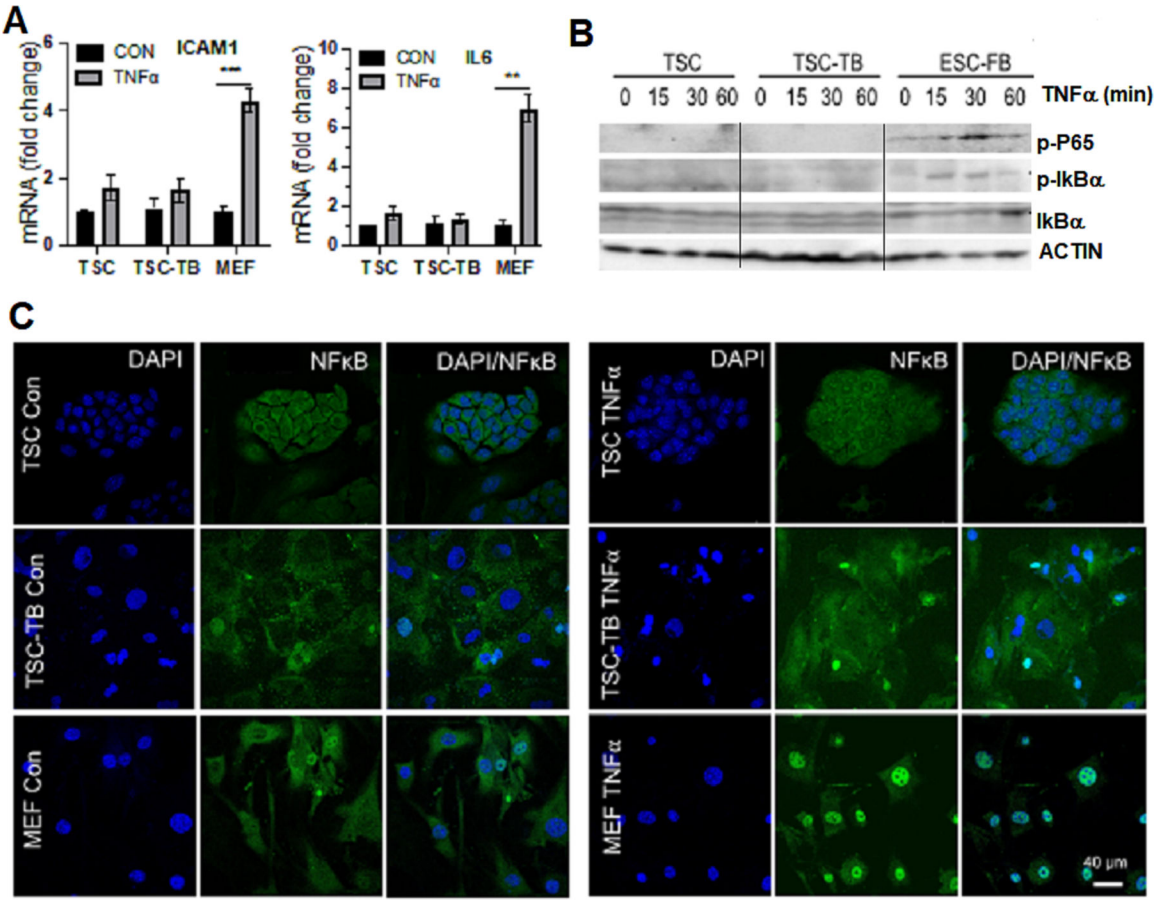

Fig. 2. TNFα-induced responses in TSCs, TSC-TBs, MEFs, and ESC-FBs.

A, Cells were treated with TNFα for 12 h. The mRNA levels of *Icam1* and *Il6* were determined by RT-qPCR. The values are mean ± SD (n=3). P<0.001, ***; P<0.01, ** compared with the control group. **B,** Western-blot analysis of the effects of TNFα on p-p65, p-IκBα, and IκBα. ACTIN was used as a loading control. **C**, Nuclear localization of NFκB. Cells were treated with TNFα for 30 min or left untreated (Con). The cellular location of NFκB was determined with an antibody against the p65 subunit of NFκB and detected with FITC-conjugated secondary antibodies. Nuclei were stained with DAPI. DAPI/NFκB represents the merged image of NFκB and DAPI staining. Scale bar = 40 μm.

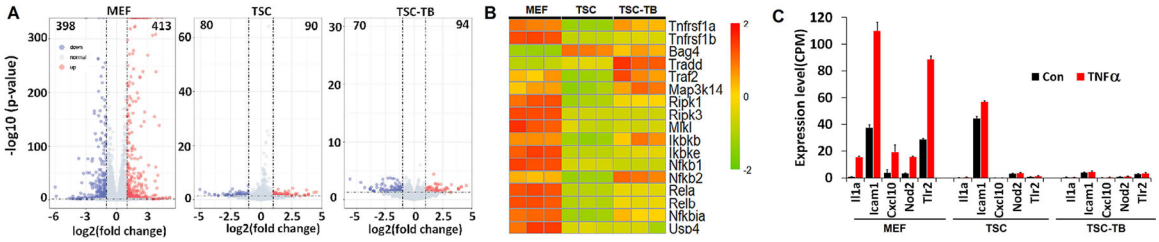

Fig.3. TNFα-induced responses in MEFs, TSCs, and TSC-TBs determined from RNA-seq.

A, Volcano plot of DEGs in MEFs, TSCs, and TSC-TBs induced by TNFα. The X-axis represents the fold change in expression levels between TNFα-treated cells relative to control cells for each transcript in a log2 scale. The Y axis indicates the statistical significance expressed as −log10 (p value) from the simple comparison. Transcripts with a log2 difference ≥1 and with p≤0.05 were defined as DEGs. **B,** Heat map representation of relative expression levels of selected signaling molecules in the TNFα pathway in MEFs, TSCs, and TSC-TBs. The color spectrum, ranging from red to green, indicates high to low normalized levels of expression of each gene. **C.** The expression levels of representative TNFα-induced genes. The values are mean ± SD (n=3) calculated from RNA-seq analysis (CPM).

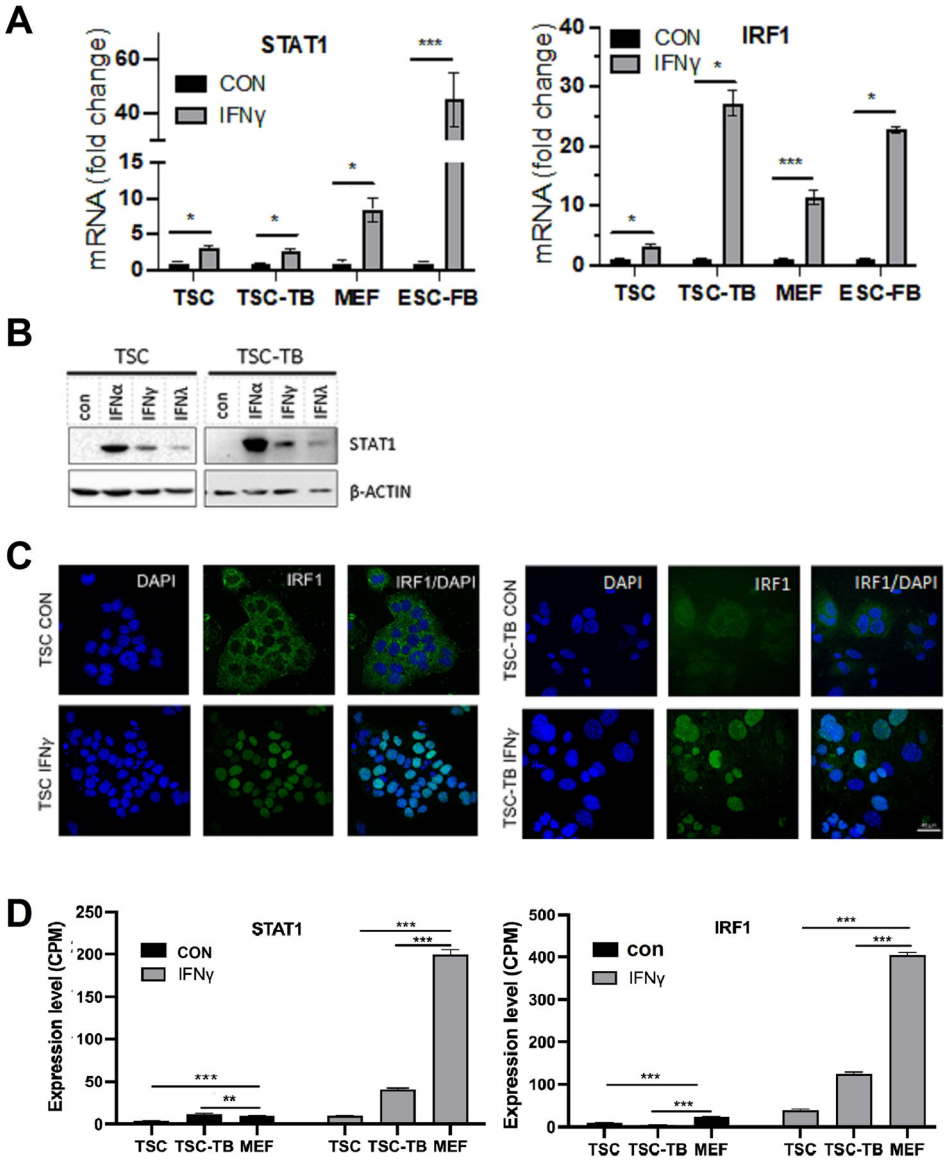

Fig.4. IFNγ-induced expression of STAT1 and IRF1.

A, Cells were treated with IFNγ for 12 h. The mRNA levels of *Stat1* and Irf1 were determined by RT-qPCR in control cells (CON) and IFNγ treated cells (IFNγ). The values are mean ± SD (n=3). P<0.001, ***; P<0.05, * compared with control groups. **B,** Western-blot analysis of STAT1 expression in the cells treated with IFNγ, IFNα, or IFNλ for 24 h or untreated cells (Con). ACTIN was used as a loading control. **C,** IFNγ-induced IRF1 expression was detected in the nuclei by immunostaining with anti-IRF1 antibodies. Nuclei were stained with DAPI. IRF1/DAPI represents the merged image of IRF1 and DAPI staining. Scale bar = 40 μm. D. The relative expression levels of STAT1 and IRF1 in control (CON) and cells treated with IFNγ (IFNγ) for 12 h. The values are mean ± SD (n=3) calculated from RNA-seq analysis (CPM). P<0.001,***; P<0.01,** compared with MEFs in each group.

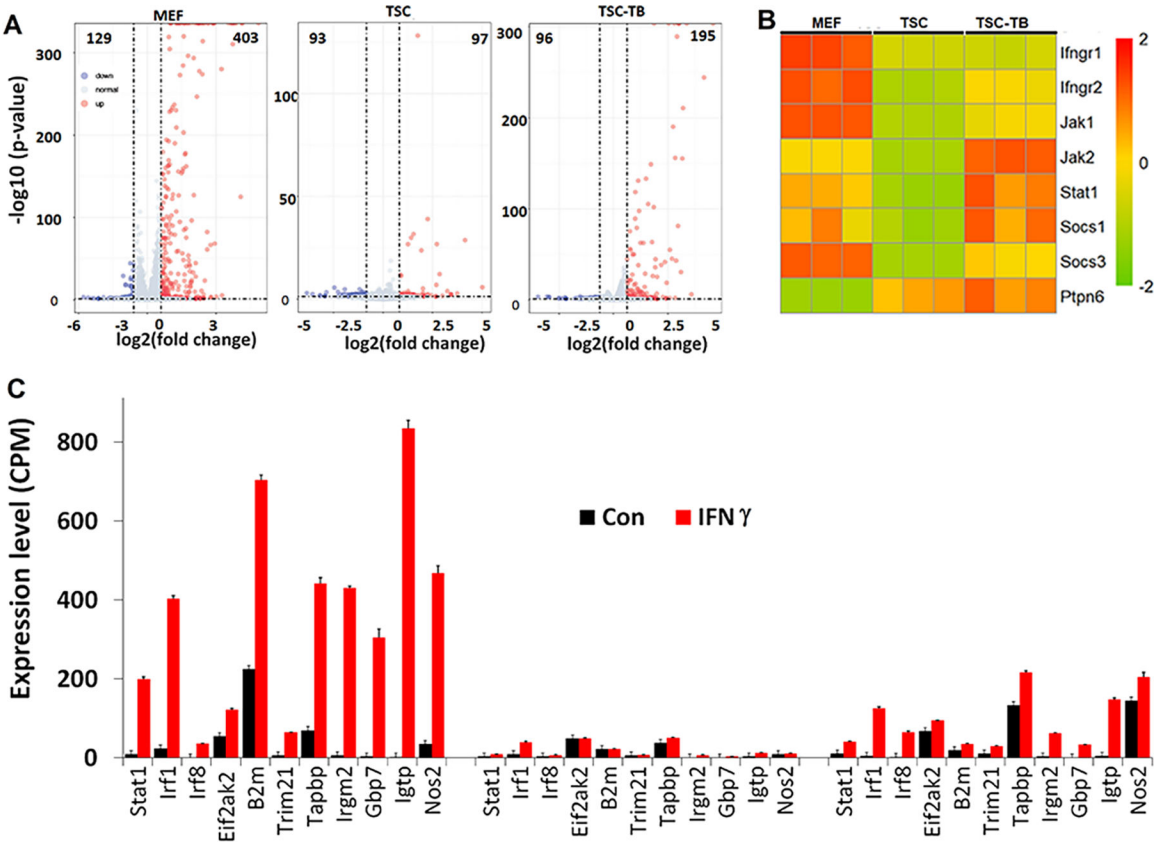

Fig. 5. IFN γ responses in MEFs, TSCs, and TSC-TBs.

A, Volcano plot of DEGs in MEFs, TSCs, and TSC-TBs induced by IFN γ. The X-axis represents the fold change in expression levels between IFN γ-treated cells relative to control cells for each transcript in a log2 scale. The Y axis indicates the statistical significance expressed as −log10 (p value) from the simple comparison. Transcripts with a log2 difference ≥1 and with p≤0.05 were defined as DEGs. **B**, Heat map representation of relative expression levels of the key signaling molecules in the IFN γ signaling pathway in MEFs, TSCs, and TSC-TBs. The color spectrum, ranging from red to green, indicates high to low normalized levels of expression of each gene (n=3). **C.** The expression levels of representative IFN γ-induced genes were calculated from CPM determined from RNA-seq data. The values are mean ± SD (n=3).

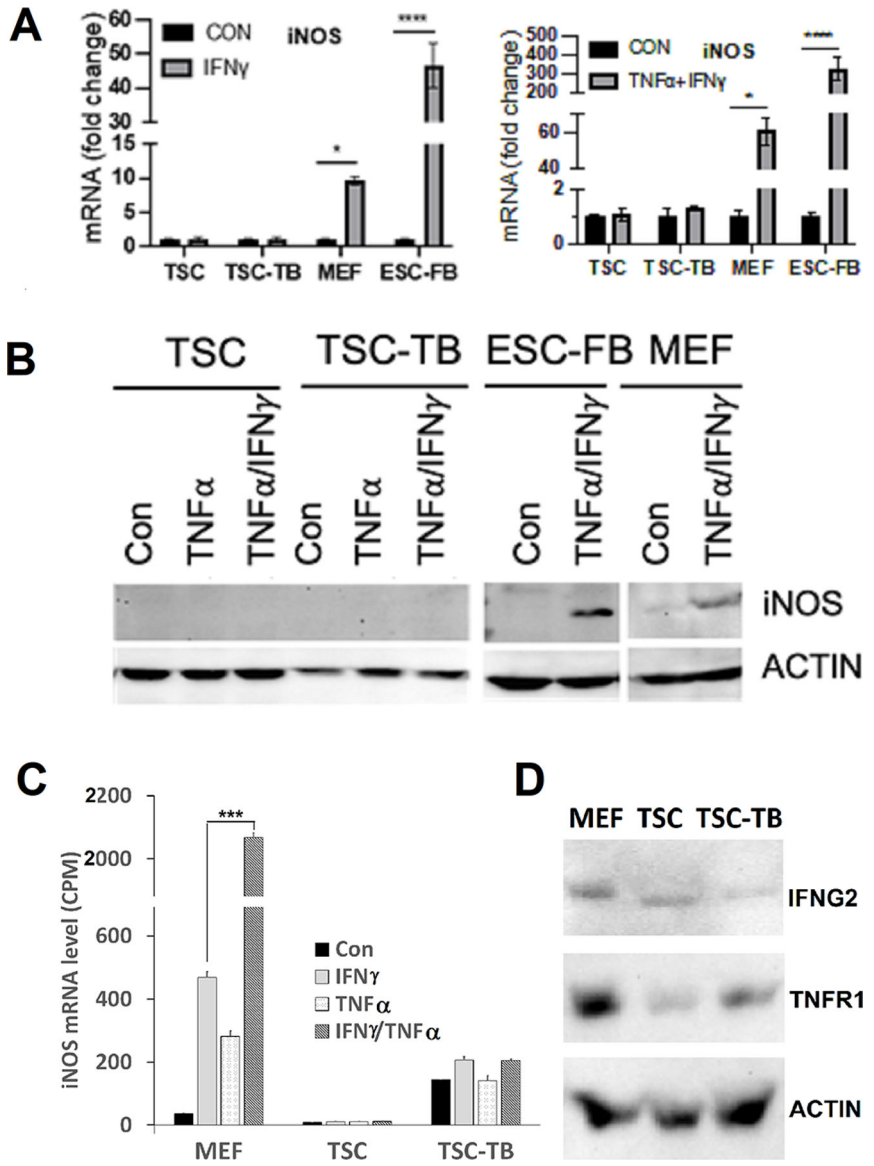

Fig.6. TNFα and IFNγ synergistically induced iNOS expression in MEFs and ESC-FBs but not in TSCs and TSC-TBs.

A, Cells were treated with IFNγ or TNFα/FNγ for 12 h. The mRNA levels of *Nos2* were measured by qPCR. **B**, Cells were treated with indicated cytokines for 24 h. The protein levels of iNOS were determined by Western-blot analysis. ACTIN was used as a loading control. **C**, The expression levels of iNOS were determined from RNA-seq analysis (CPM). Values are mean ± SD (n=3). P<0.001,*** Compared groups are indicated by a horizontal bar. D, Western-blot analysis of TNFR1 and IFNGR2 expression in MEFs, TSCs, and TSC-TBs. ACTIN was used as a loading control. Western-blot analysis was performed two times using samples prepared from five independent experiments. The blots shown are representative of the two experiments with similar results.

Table I.

PCR primers used in this study

Gene	Sequence (forward)	Sequence (reverse)
β-actin	CATGTACGTAGCCATCCAGGC	CTCTTTGATGTCACGCACGAT
ICAM1	GGCATTGTTCTCTAATGTCTCCG	GCTCCAGGTATATCCGAGCTTC
IL6	TAGTCCTTCCTACCCCAATTTCC	TTGGTCCTTAGCCACTCCTTC
NOS2	CAGCACAGGAAATGTTTCAGC	TAGCCAGCGTACCGGATGA
STAT1	CTGCCTATGATGTCTCGTTT	TGCTTTTCCGTATGTTGTGCT
IRF1	ATGCCAATCACTCGAATGCG	TTGTATCGGCCTGTGTGAATG